CellPress

Cell Stem Cell
Article

Oncogenic Amplification of Zygotic Dux Factors in Regenerating p53-Deficient Muscle Stem Cells Defines a Molecular Cancer Subtype

Jens Preussner,[1,2,8] Jiasheng Zhong,[1,8] Krishnamoorthy Sreenivasan,[1] Stefan Günther,[1,3] Thomas Engleitner,[4] Carsten Künne,[1,2] Markus Glatzel,[5] Roland Rad,[4] Mario Looso,[2] Thomas Braun,[1,6,7] and Johnny Kim[1,6,9,*]

[1]Department of Cardiac Development and Remodeling, Max-Planck-Institute for Heart and Lung Research, Bad Nauheim, Germany
[2]Bioinformatics Core Unit (BCU), Max Planck Institute for Heart and Lung Research, Bad Nauheim, Germany
[3]ECCPS Deep Sequencing Platform, Max Planck Institute for Heart and Lung Research, Bad Nauheim, Germany
[4]Institute of Molecular Oncology and Functional Genomics, Translatum Cancer Center and Department of Medicine II, Technical University of Munich, Munich, Germany
[5]Institute of Neuropathology, University Medical Center Hamburg-Eppendorf, Hamburg, Germany
[6]German Center for Cardiovascular Research (DZHK), Rhine Main, Germany
[7]German Center for Lung Research (DZL), Giessen, Germany
[8]These authors contributed equally
[9]Lead Contact
*Correspondence: johnny.kim@mpi-bn.mpg.de
https://doi.org/10.1016/j.stem.2018.10.011

SUMMARY

The identity of tumor-initiating cells in many cancer types is unknown. Tumors often express genes associated with embryonic development, although the contributions of zygotic programs to tumor initiation and formation are poorly understood. Here, we show that regeneration-induced loss of quiescence in p53-deficient muscle stem cells (MuSCs) results in rhabdomyosarcoma formation with 100% penetrance. Genomic analyses of purified tumor cells revealed spontaneous and discrete oncogenic amplifications in MuSCs that drive tumorigenesis, including, but not limited to, the amplification of the cleavage-stage Dux transcription factor (TF) Duxbl. We further found that Dux factors drive an early embryonic gene signature that defines a molecular subtype across a broad range of human cancers. Duxbl initiates tumorigenesis by enforcing a mesenchymal-to-epithelial transition, and targeted inactivation of Duxbl specifically in Duxbl-expressing tumor cells abolishes their expansion. These findings reveal how regeneration and genomic instability can interact to activate zygotic genes that drive tumor initiation and growth.

INTRODUCTION

The cell of origin for many cancer types remains unknown, although the hypothesis has been put forward that cancerous stem cells (CSCs) typically arise out of healthy stem cells. In support of this hypothesis, prevalent types of cancer most often occur in tissues containing cells with increased proliferative potential inferred by tissue resident stem cells (SCs), which normally enable regeneration of the respective tissue (Morrison and Spradling, 2008; Tomasetti and Vogelstein, 2015). An excellent example and experimentally tractable model to study stem-cell-dependent regeneration is that of skeletal muscle, which is mediated by and dependent on rare Pax7-expressing muscle SCs that reside between the basal lamina and plasma membrane of mature skeletal muscle fibers (Almada and Wagers, 2016; Günther et al., 2013). Under resting conditions, muscle SCs are predominantly quiescent but become activated upon regenerative cues, such as an inflicting injury or during chronic regeneration of certain diseases. For example, muscle SCs from mdx mice that mimic certain features of Duchenne muscular dystrophy undergo continuous activation due to persistent muscle fiber degeneration and the consequent requirement for *de novo* fiber formation under steady-state conditions (Boldrin et al., 2015).

Recently, it was shown that germline inactivation of the tumor suppressor p53 in chronically regenerating mdx mice develop rhabdomyosarcoma (RMS) (Camboni et al., 2012; Chamberlain et al., 2007), a rare and aggressive childhood cancer and the most common soft-tissue sarcoma in children and adolescents (El Demellawy et al., 2017). The cancer cell of origin of RMS has yet remained unclear, in particular under these settings, although forced expression of common potent oncogenic drivers in muscle SCs, including, but not limited to, *kras* or *yap1*, can result in RMS formation (Blum et al., 2013; Chen et al., 2013; Hettmer et al., 2011; Shern et al., 2014; Tremblay et al., 2014). Other reports have indicated RMS to originate in mesenchymal cells (Wang et al., 2014), and it was recently demonstrated that RMS can arise through malignant myogenic trans-differentiation of endothelial progenitors via activation of the hedgehog pathway (Drummond et al., 2018). Indeed, RMS tumors are generally thought of as skeletal muscle tumors because they display features of myogenic differentiation reflected by the expression of myogenic determinants, such as MyoD, MyoG, and Desmin, all of which are sequentially expressed in activated muscle SCs during the progression of adult muscle regeneration and in muscle progenitors during

embryonic muscle development (Almada and Wagers, 2016; Braun and Gautel, 2011). Incidentally, the notion has been raised that re-expression of genes normally expressed in tissue-specific progenitors during embryonic development might be responsible for the stem-cell-like phenotypes of various poorly differentiated human tumors, including RMS, germ cell tumors, breast cancer tumors, glioblastoma, and bladder cell carcinoma (Ben-Porath et al., 2008). However, in which cell types, how, and by what means embryonic gene expression programs would be elicited to induce tumor formation and whether or not any of these associated genes are causally transformative has remained largely unknown.

Genomic sequencing of tumors from patients suffering from RMS and many other types of cancer has unveiled oncogenic mutations and copy number (CN) gains of certain genes associated with tumor formation (Chen et al., 2013; Editorial, 2015 [in *Nature Medicine*]; Shern et al., 2014). However, for most patients, both the specific cellular and genetic etiologies of tumor formation remain unknown, illustrating that mechanisms of tumorigenesis remain to be identified and by more refined methods. The constant proliferative and regenerative pressure on the muscle SC compartment in continuously regenerating mdx mice led us to reason that muscle SCs could be a cellular origin of RMS tumors. Here, we devised an inducible strategy (1) to clarify the cellular origin of RMS tumors, (2) to delineate the causal role of stem-cell-dependent regeneration in cancer progression, and (3) that would enable identification of causative mechanisms, leading to tumorigenic transformation of healthy stem cells *in vivo*.

RESULTS

Lineage Tracing Identifies Muscle SCs as a Cellular Origin of Embryonic RMS

To investigate the cell-autonomous role of muscle SCs in RMS formation, we generated mice that enable muscle-SC-specific deletion of p53 in both wild-type and constitutively regenerating mdx mice by intraperitoneal administration of tamoxifen (TAM), designated hereafter as SC^{p53} and $SC^{p53/MDX}$, respectively. We additionally introduced a Rosa26::lsl Tomato allele enabling permanent fluorescent lineage tracing of SCs after TAM treatment (Figure 1A). Strikingly, 20 weeks after TAM treatment, all $SC^{p53/MDX}$ mice developed tumors in, or immediate proximity to, the musculature of extremities or the trunk and were all histopathologically classified as embryonic RMS immunopositive for Desmin, MyoD, and MyoG (Figures 1A–1C and S1A). Remarkably, some mice developed several tumors; however, TAM-treated wild-type, mdx, or SC^{p53} mice never developed tumors up to an age of more than 52 weeks (Figure 1B). Consecutive bouts of cardiotoxin (CTX)-induced injury to the tibialis anterior (TA) muscle of SC^{p53} mice uniformly resulted in RMS formation at the site of injury, whereas control animals never developed tumors (Figure S1B). These data show that muscle-SC-specific loss of p53 in a regenerative environment is sufficient to generate RMS, or conversely, that a regenerative environment enables RMS formation upon muscle-SC-specific loss of p53. Moreover, these data support the notion that maintenance of SC quiescence provides a cellular mechanism to suppress tumorigenesis and are consistent with previous reports demonstrating that muscle injury is required to elicit RMS formation upon forced overexpression of oncogenic drivers, such as yap1 (Tremblay et al., 2014). All of the tumors were lineage traced by activation of the Rosa26-Tomato locus, clearly indicating muscle SCs as the cellular origin of the RMS tumors in these animals (Figure 1C). Consistently, strong Tomato fluorescence of the skeletal muscle, but not the liver, revealed prominent and specific contribution of muscle SCs toward *de novo* myofiber formation, as expected in chronically regenerating mdx muscles and over the period before tumor onset (Figure 1C). We next obtained single cell isolates from surgically excised skeletal muscles and tumors and subjected them to fluorescence-activated cell sorting (FACS), enabling separation and purification of muscle SCs and both lineage-traced and non-lineage-traced tumor-propagating cells (TPCs), respectively (Figures 1D, S1C, and S1D). PCR-based genotyping, immunofluorescent staining, and qRT-PCR of isolated tissues and FACS-purified SCs and TPCs confirmed that recombination of the p53 locus was highly efficient and specific to muscle SCs and disclosed that purified Tomato-positive cells were strictly deficient for p53 and purified Tomato negative cells only contained non-recombined p53 DNA (Figures 1E and S1C–S1F). In addition, immunofluorescent staining and qRT-PCR of the freshly isolated SCs revealed that chronic regeneration elicits expression of p53 in a subset of SCs, albeit at low levels (Figures S1E–S1G). Notably, regenerated skeletal muscles still contained DNA with intact p53 alleles, most likely reflecting the presence of myofibers derived from muscle SCs before and after the onset of p53 deletion and/or other muscle-resident cells. Likewise, DNA isolated from bulk tumors contained DNA with both intact and recombined p53 alleles (Figure 1E), in agreement with the observation that the tumors consisted of lineage-traced and non-lineage-traced TPCs (Figures 1C and 1D). These data demonstrate (1) the specific contribution of Pax7-expressing muscle SCs toward RMS formation and (2) the complex cellular composition of the developing tumors containing cells that are and are not derived from Pax7-expressing SCs. Essentially, FACS-separated TPCs were either strictly $p53^{+/+}Tom^{neg}$ or $p53^{-/-}Tom^{pos}$ (Figures 1D and 1E) that did or did not express myf5, myod, or myog, respectively, further confirming efficient labeling of $p53^{-/-}$ muscle SCs (Figure 1F). In contrast to $p53^{-/-}Tom^{pos}$ cells, $p53^{+/+}Tom^{neg}$ cells were highly enriched for cdkn1a mRNA transcripts (also known as p21), a primary target of p53 (Figure 1F), emphasizing that the loss of p53 functions in RMS formation specifically in muscle-SC-derived cells expressing myogenic markers. Importantly, only transplantation of $p53^{-/-}Tom^{pos}$, but not $p53^{+/+}Tom^{neg}$, cells into immunocompromised mdx-nude mice generated tumors at the site of injection already two weeks after transplantation (Figures 1G and 1H). Taken together, these data demonstrate that lineage tracing enables prospective purification of genuine tumor-propagating cells clearly originating from muscle SCs that are responsible for tumor formation.

Genomic Analyses of Purified TPCs

To gain insight on the molecular mechanism leading to transformation of SCs, we next analyzed proliferation and differentiation of wild-type, mdx, p53, and p53/mdx muscle SCs *in vitro*. Inactivation of p53 and/or dystrophin in muscle SCs did not impair terminal myogenic differentiation upon serum withdrawal (Figure 2A). However, under growth conditions, p53-deficient

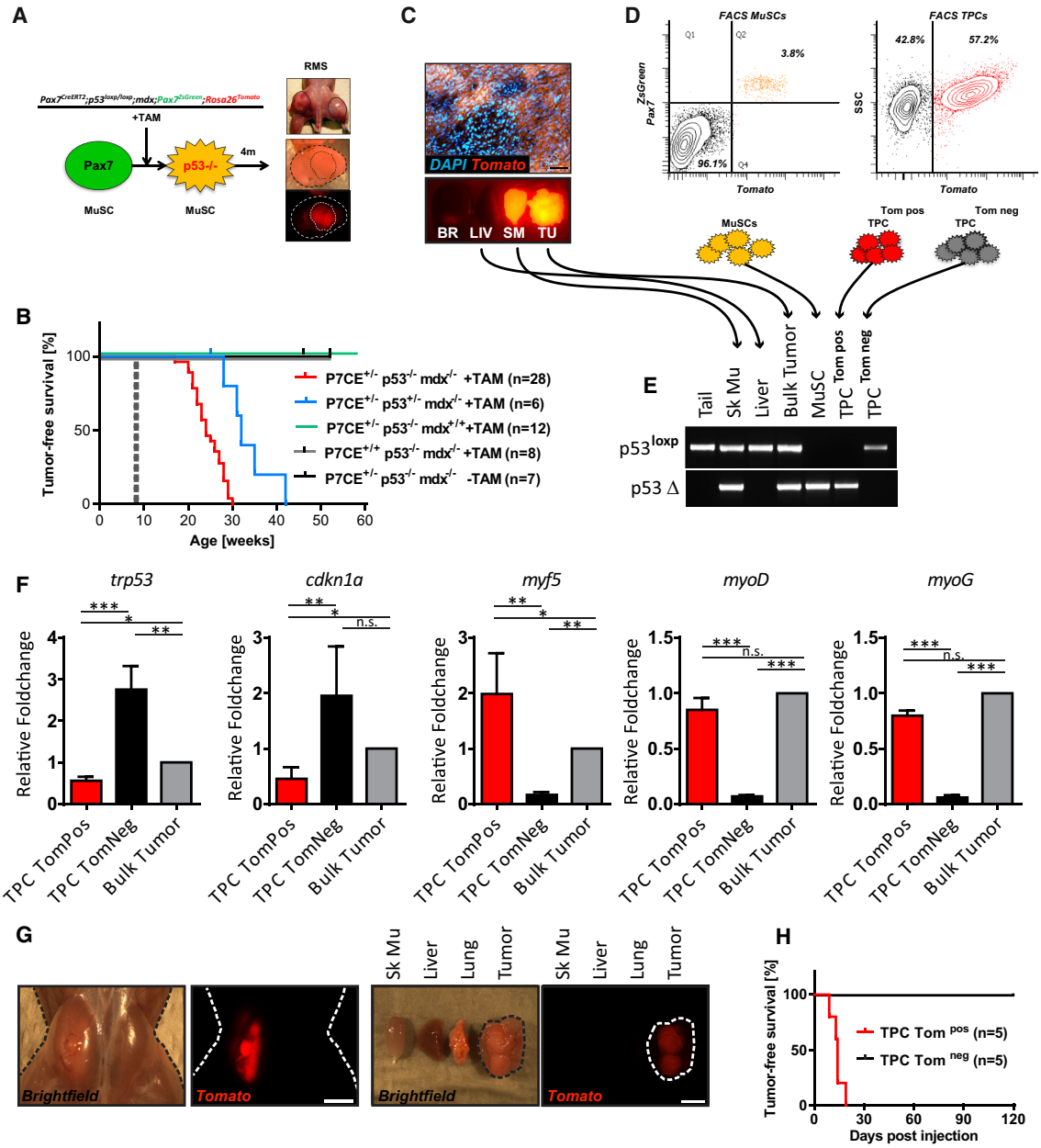

Figure 1. Loss of p53 in Muscle SCs Induces ERMS Tumors in mdx Mice

(A) Genetic components of the model system. p53 is deleted in muscle SCs expressing ZsGreen and simultaneously lineage traced *in vivo* via recombination of a Rosa26lsl::CAG^{Tomato} allele upon tamoxifen injection. Fluorescence enables FACS-based purification of muscle SCs and separation of lineage-traced and non-lineage-traced TPCs.

(B) Kaplan-Meier tumor-free survival curves are shown for indicated genotypes. Dashed line indicates timing of tamoxifen administration.

(C) Representative immunofluorescent images of isolated tissues (bottom panel) and cross-sectioned tumor (top panel). Note that not all cells within the tumor are lineage traced.

(D) FACS plots of purified SCs and TPCs.

(E) Genotyping of the p53 gene locus in indicated tissues, purified muscle SCs, and TPCs.

(F) mRNA expression analysis of p53, cdkn1a, and myogenic factors in purified TPCs and corresponding bulk tumors. Error bars indicate SD of the mean (t test: *p < 0.05; **p < 0.01; ***p < 0.001; n = 4).

(G) Macroscopic image of Tomato expression in tumors after injection of purified TPC^{TOMpos} in mdx-nude mice. Scale bar: 5 mm.

(H) Kaplan-Meier tumor-free survival curves for mdx-nude mice injected with either TPCs^{TOMpos} or TPCs^{TOMneg}.

muscle SCs displayed significantly enhanced proliferation and concomitant formation of DNA double-strand breaks (DSBs) reflected by a dramatic increase of EdU-incorporating, γH2AX, ATM, and 53bp1-positive SCs (Figures 2B–2E). These data demonstrate that loss of p53 does not impair differentiation but permits accumulation of mutations in actively proliferating

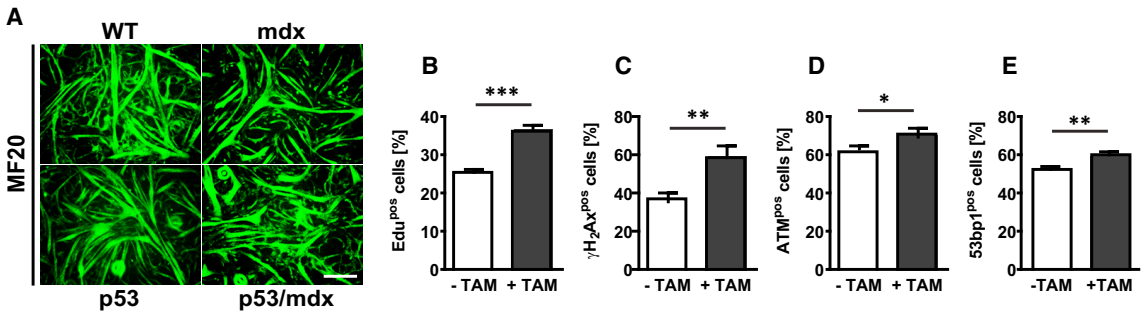

Figure 2. Loss of p53 Does Not Inhibit Myogenic Differentiation but Elicits Genomic Instability in Activated Muscle SCs

(A) Immunofluorescent staining of differentiated myotubes for indicated genotypes with MF20 antibody detecting sarcomeric actin. Scale bar: 50 μm.

(B–E) Quantification of percentage of (B) EdU, (C) γH2AX, (D) ATM, and (E) 53bp1-positive muscle SCs from $SC^{p53/mdx}$ mice in culture under growth conditions. Error bars represent SDs of the mean (t test: *p < 0.05; **p < 0.01; ***p < 0.001).

SCs, of which some might be responsible for tumorigenic transformation.

To identify mutations promoting tumor formation, we performed whole-exome sequencing on paired tumor-normal samples. Strikingly, CN analysis revealed discrete and dramatic genomic CN amplifications in almost every specimen (21 out of 22) when paired purified TPC^{TOMpos}-normal samples were used (Figures 3B–3G, S2A–S2S, S3A, and S3B). In contrast, we did not always detect CN variations when genomic DNA from bulk tumors was analyzed, demonstrating that non-tumorigenic stromal cells interfere with the analysis of genomic sequencing data (Figure 3A). Positional mapping of CN amplifications within each and across samples revealed genomic amplification of defined chromosomal regions harboring known mutational targets in ERMS, including yap1 (Tremblay et al., 2014; 8/22; 36%), c-met (Fleischmann et al., 2003; Taulli et al., 2006; 5/22; 23%), jun (Durbin et al., 2009; 1/22; 4.5%), and cdk4/gli1/os9 (Liu et al., 2014; 1/22; 4.5%). We also identified mutational targets that had not been associated with embryonic RMS (ERMS) so far but with other types of cancer, including rras (Flex et al., 2014), kdm4d (Soini et al., 2015), bap1 (Robertson et al., 2017), mcm4 (Polotskaia et al., 2015; Shima et al., 2007), and eloc (Sato et al., 2013; Figures 3F, 3G, S2A–S2S, S3A, and S3B). Several mice displayed amplification on chromosome 14qA3 (5/22; 23%), harboring a poorly described triplicated genomic locus in the mouse genome encoding for the genes plac9, tmem254, cphx, and duxbl (Figures 3D, 3F, and 3G). Notably, genomic analysis of two highly aggressive allografts, which harbored yap1/c-met and yap1/kdm4d amplifications, respectively, did not reveal significant accumulation of *de novo* mutations or CNAs two weeks after the tumor cell transplant (Figure 3F). In addition, a linkage between the amplified genes within and across samples was not detected, suggesting that, for each individual animal, a single discrete amplification was likely sufficient for SC transformation. Interestingly, we also noticed a dramatic reduction of mtDNA in many of the TPCs, suggesting those to be glycolytic and had likely undergone a Warburg effect (Figures 3B, 3D, 3E, and S2A–S2S). In contrast to oncogenic amplifications, somatic single-nucleotide variations (SNVs) were astonishingly low (Figures S4A and S4B), concordant with recent observations that soft-tissue sarcomas are predominantly characterized by copy number changes, with low mutational loads of only a few genes, including p53, atrx, and rb1 (The Cancer Genome Atlas Research Network, 2017; Chen et al., 2013; El Demellawy et al., 2017; Shern et al., 2014). Tables supporting CN and SNV analyses are provided in Tables S1 and S2.

Dux TFs Define a Molecular Subtype of Cancer

The subset of tumors containing amplification of 14qA3 was of particular interest, because this genomic region does not contain any known oncogene. We noticed that 14qA3 harbors the *duxbl* gene, which belongs to the Dux family of homeobox-containing transcription factors with human Dux4 as the founding member (Leidenroth and Hewitt, 2010). Recently it was shown that Dux4, or the murine homolog Dux, is responsible for driving cleavage-stage gene expression signatures known as zygotic gene activation (ZGA) in totipotent embryonic stem cells (ESCs) (De Iaco et al., 2017; Hendrickson et al., 2017; Whiddon et al., 2017). The human genome encodes two additional paralogs of Dux4, named DuxA and DuxB, which are expressed exclusively at the totipotent 8-cell stage in early zygotes (Madissoon et al., 2016). These observations led us to speculate that Dux transcription factors might act at a putative interface of stem cell potency and tumor formation.

To test this hypothesis, we analyzed previously published discovery cohorts of human ERMS patients (Chen et al., 2013; Davicioni et al., 2009; Williamson et al., 2010) for expression of Dux4, DuxA and DuxB, and/or ZGA. We assumed that a putative role of Dux genes in causing human ERMS might have been missed in the past due to poor annotation and in particular of the Dux family and ZGA-associated genes. In this context, it is noteworthy to mention that the human *duxA* and *duxB* genes were only recently identified and annotated, with human *duxB* being in genomic synteny with mouse *duxbl* and human *dux4* is in synteny with murine *dux* (Leidenroth et al., 2012; Leidenroth and Hewitt, 2010). Intriguingly, and consistent with the proposed role of Dux factors in driving cleavage-stage-specific gene expression signatures (Hendrickson et al., 2017), we identified 54 RMS tumors (~10%) that were strikingly positive for ZGA and/or Dux factor expression (Figures 4A and S5A–S5D; Table S3). Reanalysis of raw sequencing data of mRNA transcripts available from the dataset of Chen et al. (2013) disclosed four ZGA-positive patients of which two (X03D and X20A) expressed

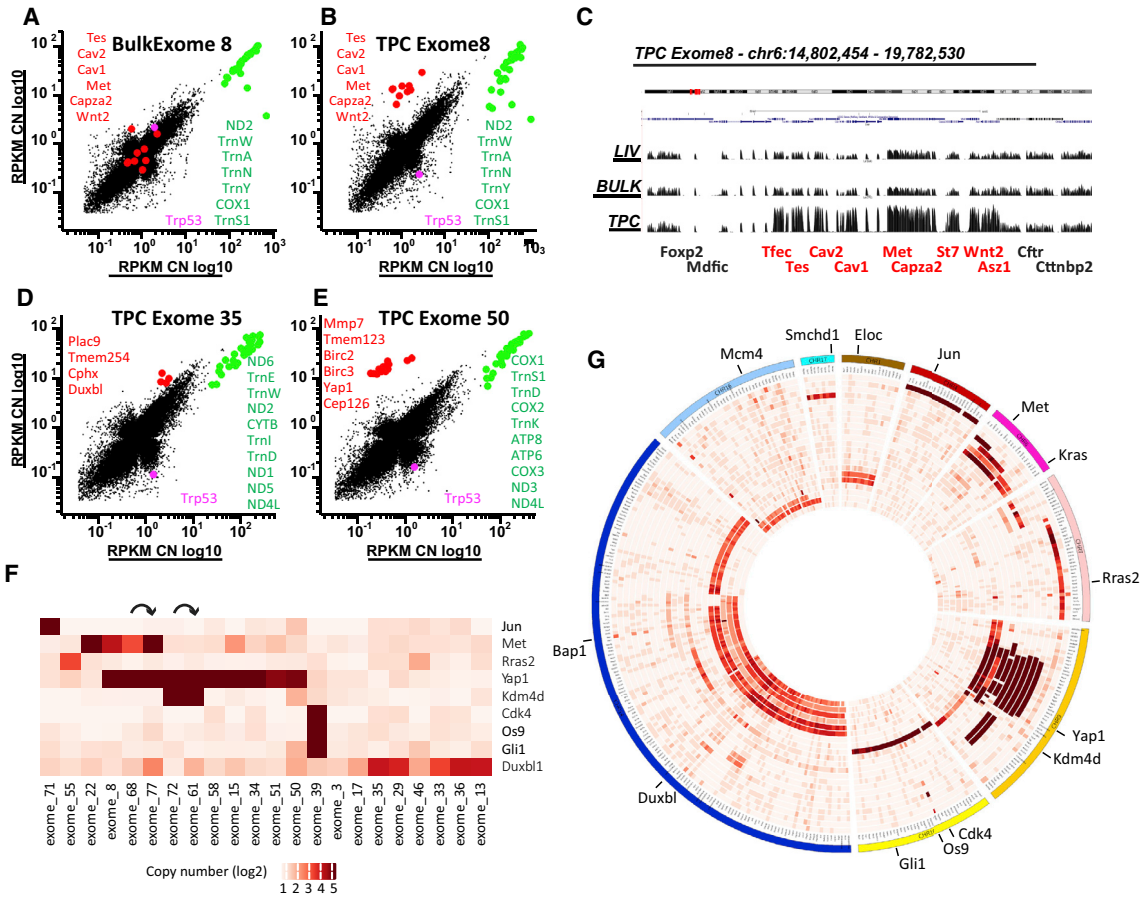

Figure 3. Identification of Distinct Copy Number Amplifications in RMS Tumors

(A, B, D, and E) Scatterplots depicting log-scaled RPKM values of genomic DNA in purified tumor cells (y axis) (B, D, and E) or in non-purified bulk tumor (A) versus liver control (x axis). Note that the same genes are highlighted in red in (A), (B), and (C). Green circles represent mitochondria-encoded genes. Red circles represent amplified genes. Magenta circle represents p53.

(C) Amplified genes highlighted in red in (A) and (B) displayed in physical genomic order.

(F) Heatmap summarizing amplified genes in the 22 analyzed tumors. Curved arrows indicate allografts of donor TPCs and TPCs after transplantation into recipient.

(G) Cumulative CIRCOS plot of amplified genes from all analyzed tumors. Note that genomic regions are displayed in physical order.

dramatically high levels of Dux4, DuxA, and DuxB (Figures 4A and S5A). These data indicate that Dux transcription-factor-driven zygotic gene activation defines a molecular signature of a new ERMS subtype. We next sought to investigate whether increased expression of Dux genes is restricted to ERMS or also associated with other malignancies. To this end, we re-screened <10,000 cancer patients of The Cancer Genome Atlas–Pan-Cancer (TCGA-PANCAN) dataset (Hoadley et al., 2014) for Dux4, DuxA, and DuxB exon expression. Intriguingly, we identified 349 patients that displayed distinct expression of Dux4, DuxA, and DuxB either in combination or alone. Cancer onset and type in these patients was highly variable, comprising of 32 different types of somatic cancer according to ICD-1O (International Classification of Diseases for Oncology) (Figure 4B; Table S3). These data show that Dux transcription factors driving early zygotic gene signatures define a molecular subtype of a broad range of human cancers.

We noticed that two tumors from the sequenced RMS cohort (X013D and X45D) displayed ZGA to a lower degree than X03D and X20A, which corresponded to clearly detectable but lower levels of Dux4, DuxA, or DuxB (Figures S5A and S5B). Similar expression patterns were visible in the larger cohort of patients from the PANCAN dataset, supporting the idea that Dux factors act upstream of ZGA to initiate tumorigenesis but that sustained Dux-mediated ZGA may not be required for maintenance of established tumors. Notably, tumors showing the most striking expression of Dux4, DuxA, DuxB, and ZGA were predominantly classified as testicular germ cell carcinomas (TGCs), more than half of which developed in subjects younger than 20 years old, thus indicating a particular vulnerability of Dux-ZGA–associated tumorigenesis in germ cell tissues (Figure 4C; Tables S3 and S4). Conspicuously, the most prevalent cancer types across the 349 patients (testis, breast, kidney, stomach, and lung) are thought to be of epithelial origin, and virtually all of the ZGA-positive tumors displayed prominent levels of Dux4, DuxA, and/or DuxB, but not vice versa (Figures 4B–4D, S6A, and S6B). Particularly apparent was that almost all of the breast cancer patients expressed dramatic levels of DuxB-Duxbl, but only few were additionally positive for ZGA,

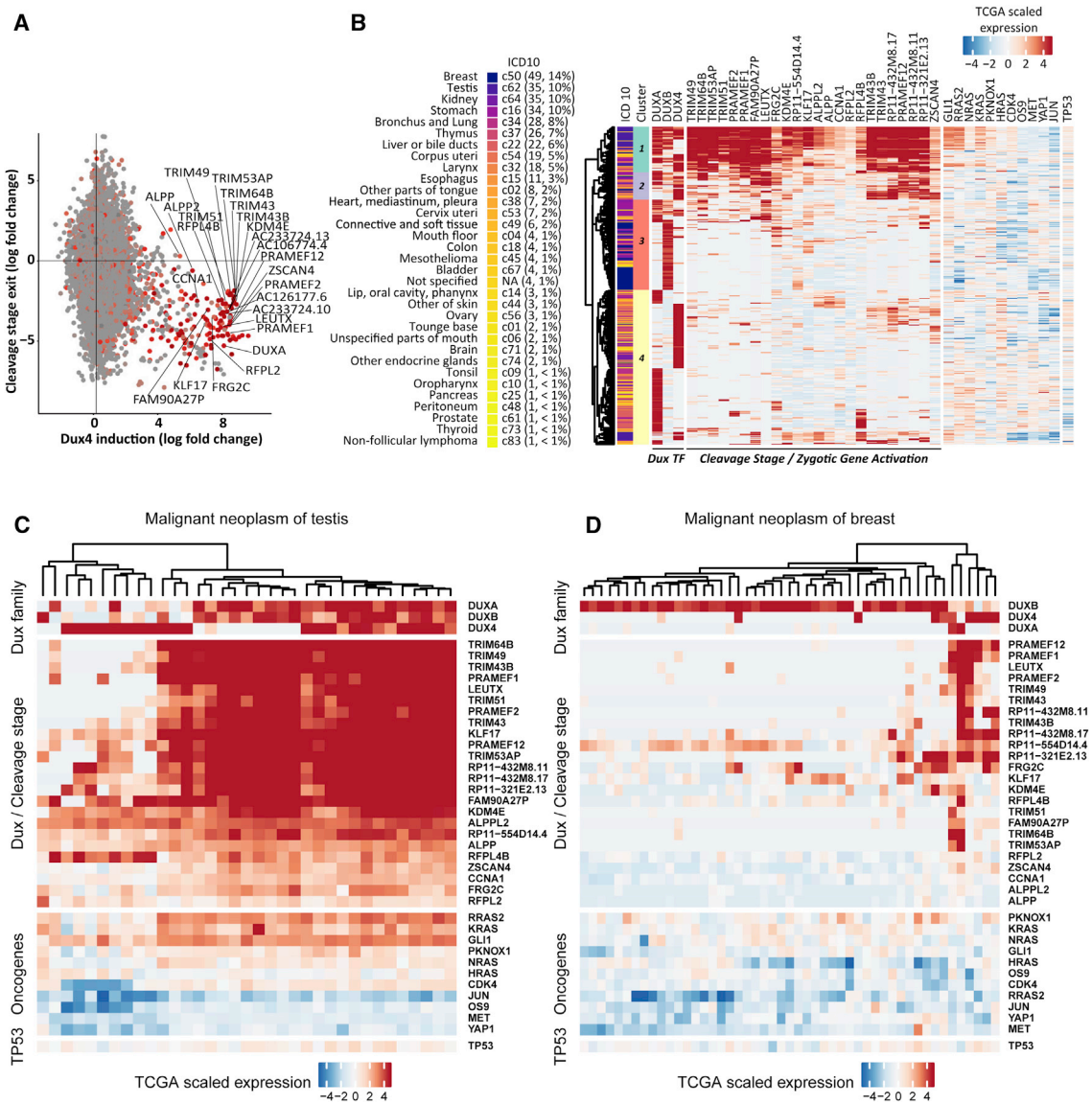

Figure 4. Dux Transcription Factors Define a Molecular Subtype of Cancer

(A) Integration analysis of Dux-dependent zygotic gene expression (x axis) and cleavage-stage-specific gene expression (y axis) in tumor from ERMS patient X20A.

(B) Unsupervised cluster analysis of tumors from the full TCGA-PANCAN dataset revealing four subgroups driven by mRNA expression of Dux factors and/or Dux-dependent zygotic gene activation. Percentages indicate prevalence of color-coded tumor type across 349 Dux-factor-ZGA–positive tumors. Clinical metadata of tumors stratified by age, gender, and cluster are provided in Tables S3 and S4.

(C and D) Unsupervised cluster analysis of breast cancer (C) and testicular germ cell carcinoma (D) positive for expression of Dux factors and/or Dux-dependent zygotic gene activation.

DuxA, and/or Dux4, suggesting Dux4 to act genetically upstream of DuxB (Figure 4D). Consistent with this hypothesis, acute overexpression of Dux4 elicited a profound and significant upregulation of ZGA-associated genes, as previously reported, and additionally DuxA and DuxB in human embryonic kidney cells (Figure S7A; Table S5; Hendrickson et al., 2017). Taken together, these data raise the idea that (1) Dux factors initiate tumorigenesis via activation of ZGA and/or (2) that Dux factor expression, and in particular DuxB-Duxbl, might facilitate tumorigenesis by an additional ZGA-independent mechanism.

Duxbl Initiates Tumor Formation via Eliciting a Mesenchymal-to-Epithelial-Transition-like Program

To gain a mechanistic understanding on the action of DuxB-Duxbl, we overexpressed Duxbl in wild-type muscle SCs via lentiviral transduction (Figure 5A). In wild-type control muscle SCs (designated hereafter as SC^{WT}), serial passaging resulted in exhaustion of proliferation concomitant with progressive formation of flattened myoblasts that robustly fused to form terminally differentiated myotubes (Figures 5B–5D). In striking contrast, overexpression of Duxbl resulted in the emergence of

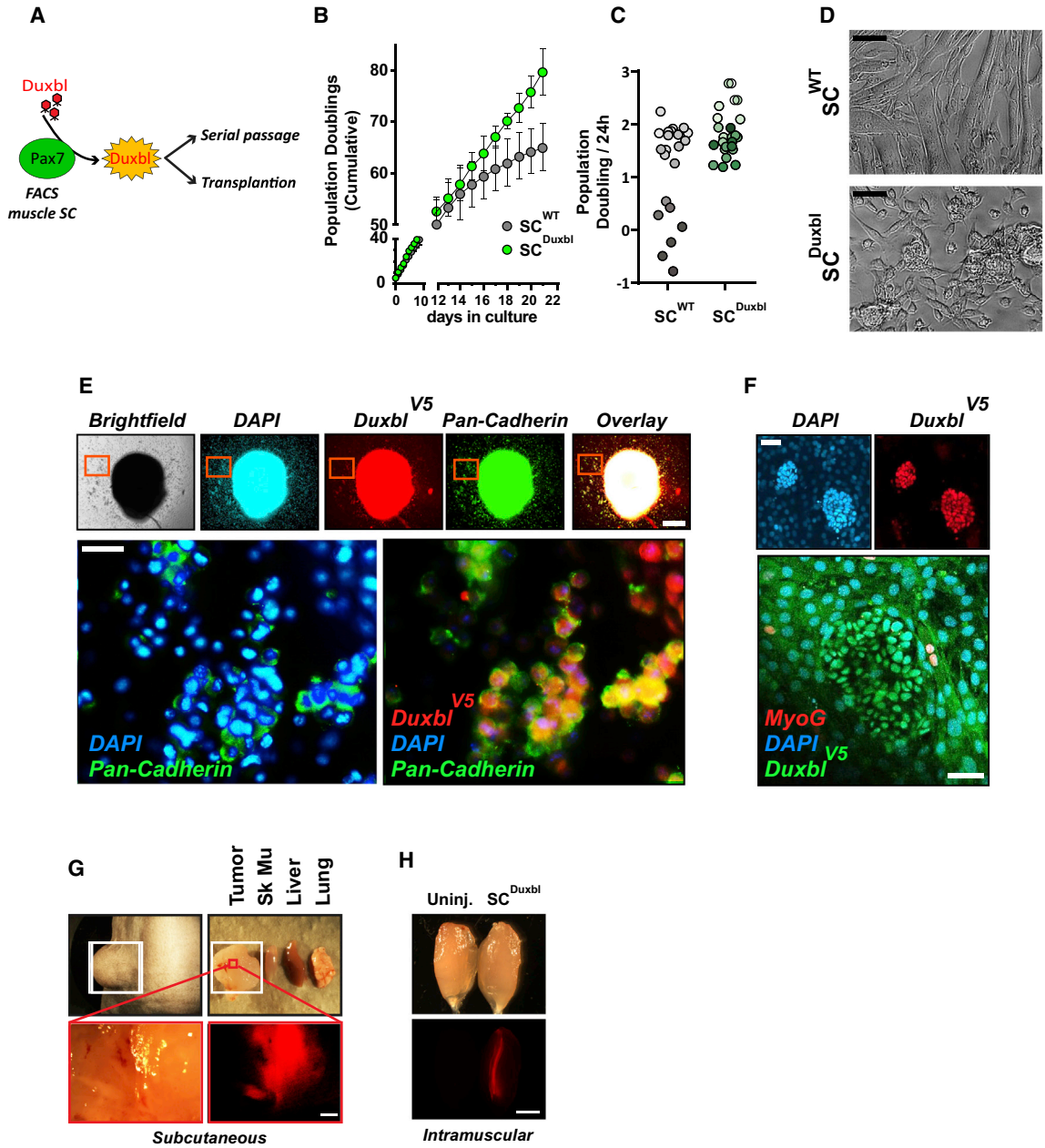

Figure 5. Overexpression of Duxbl Confers Plasticity and Promotes Tumor Formation

(A) Schematic of lentiviral-mediated transduction of V5-tagged Duxbl into wild-type (WT) muscle SCs.

(B) Cumulative population doublings over three weeks of culture. Error bars indicate SD of the mean.

(C) Population doubling rate calculated as PD = log(N1/N0)log2, where N1 is the final cell number and N0 is the initial number of seeded cells. Darker shading indicates increasing days in culture.

(D) Representative images of SCs^{WT} and SCs^{Duxbl} after 3 weeks in culture. Scale bars: 50 μm.

(E and F) Pseudo-colored immunofluorescent staining of SC^{Duxbl} colonies as indicated. Scale bars: 100 μm in top panels and 20 μm in lower panels of (E), and 20 μm in top panels and 50 μm in lower panels of (F).

(G and H) Macroscopic image of mCherry expression after injection of SC^{Duxbl} carrying an additional mCherry reporter (G) subcutaneously or (H) in TA muscle. Scale bar: 100 μM in (G) and 1 mm in (H).

immortalized and morphologically rounded clones prone to spontaneously form cadherin-positive, epithelial-like spherical aggregates that were devoid of myogenic differentiation and could be passaged indefinitely *in vitro* (designated hereafter as SC^{Duxbl}; Figures 5B–5F). Importantly, subcutaneous transplantation of SC^{Duxbl} resulted in tumor formation at the site of engraftment, clearly demonstrating that overexpression of Duxbl is sufficient for neoplastic transformation *in vivo* (Figure 5G). In

contrast, SC^{WT} did not give rise to any detectable neoplasias 3 months after subcutaneous transplantation as previously reported (data not shown; Irintchev et al., 1998). Interestingly, SC^{Duxbl} contributed to myofiber formation when injected directly into the strong pro-differentiation environment of TA muscle (Figure 5H). Collectively, these data provided an additional important mechanistic insight: it appeared that forced expression of Duxbl renders SCs to obtain increased plasticity and that the ability of SC^{Duxbl} to form tumors requires sustained reduction of pro-differentiation cues *in vivo*.

To gain a deeper molecular insight on how Duxbl might confer such plasticity, we performed RNA sequencing (RNA-seq) and compared gene expression profiles of isolated SC^{Duxbl} clones to various stages of myogenic differentiation of SC^{WT}. Linear principal-component analysis (PCA) revealed that separation of conditions (PC1; explaining 33.9% of variance) was primarily driven by differential expression of genes related to stem cell maintenance and differentiation (e.g., quiescent SC^{WT} expressed Pax7, but not MyoG, in comparison to differentiated SC^{WT} and vice versa; Figures 6A–6C). Notably, SC^{Duxbl} did not express any myogenic determinants, including Myf5, Myod, or MyoG, further demonstrating that forced expression of Duxbl profoundly impairs muscle SC differentiation. Intriguingly, separation of conditions across the second dimension (PC2; explaining 26.4% of variance) was enforced by dramatic expression of genes driving epithelialization (Figures 6A–6C). Indeed, pairwise differential expression analysis of SC^{Duxbl} with all stages of muscle SC differentiation (false discovery rate [FDR] < 0.01) followed by gene set enrichment analysis (GSEA) revealed a dramatic induction of genes involved in focal adhesion and proliferation of epithelial cells (Figures 6D–6F and S7B–S7D; Table S6). Consistently, SC^{Duxbl} revealed a dramatic upregulation or induction of numerous genes encoding for integrins, collagens, and most prominently cadherins and proto-cadherins (Figures 6C and S6B–S6D). Most intriguingly, SC^{Duxbl} expressed high levels of the neural and pluripotency factor *sox2*, which was expectedly absent in all stages of SC^{WT}. Interestingly, and similar to neural stem cells, undifferentiated quiescent SC^{WT} expressed high levels of the pluripotency factor *klf4* (Kim et al., 2009), the expression of which was downregulated during differentiation of SC^{WT} but sustained in SC^{Duxbl} (Figures 6A and 6C). Notably, both *sox2* and *klf4* are instrumental to facilitate an essential mesenchymal-to-epithelial transition (MET) event during reprogramming of somatic cells to induced pluripotent stem cells (iPSCs) (Li et al., 2010). In aggregate, these data indicate that forced expression of Duxbl most likely initiates tumorigenic transformation and colonization via a mechanism similar to MET (Figure 6G).

Targeting Oncogenic Duxbl

Finally, we sought out to test whether inactivation of DuxB-Duxbl could serve as a potential target in the primary tumor cells purified from the $SC^{p53/MDX}$ mice. To this end, we carried out short hairpin RNA (shRNA)-mediated knockdown in early passaged TPCs purified from primary tumors harboring either Duxbl (TPC^{Duxbl}) or Yap1 (TPC^{Yap1}) CN amplifications. Notably, expression of Duxbl mRNA was solely found in TPC^{Duxbl}, but not in TPC^{Yap1}. Likewise, expression of yap1 was restricted to TPC^{Yap1} (Figure 7A). Strikingly, shRNA-mediated knockdown of Duxbl in TPC^{Duxbl}, but not in TPC^{Yap1}, and vice versa, resulted in cell death, demonstrating that Duxbl expression is required specifically for maintenance of TPC^{Duxbl} *in vitro* (Figures 7B and 7C; related videos on Mendeley Data at https://doi.org/10.17632/7g2pbbrn4m.1). Collectively, these data demonstrate that DuxB-Duxbl can be targeted in tumor cells but disease-causing mutations in each individual tumor need to be identified before specific therapeutic intervention.

DISCUSSION

Genetic factors and certain environmental factors, such as exposure to viruses, radiation, or other carcinogens, are known to increase the risk of cancers, but for most cases, the cellular origin and cause of cancer remains unknown. Variation of cancer risk across tissues might be explained by the number of divisions of tissue-resident stem cells (Tomasetti and Vogelstein, 2015), which differs depending on developmental stages. In support of this claim, loss of p53 in muscle SCs only resulted in ERMS formation in mice undergoing continuous skeletal muscle regeneration and with astonishingly low variation of latency.

Interestingly, p53 single-knockout mice rarely develop rhabdomyosarcomas (Donehower et al., 1992), and although chronically regenerating mdx mice display elevated levels of DNA damage under steady-state conditions, their predisposition to spontaneously develop rhabdomyosarcomas predominantly occurs after more than one year of age (Camboni et al., 2012; Chamberlain et al., 2007). Previous observations revealing that compound p53/mdx germline knockouts almost only develop rhabdomyosarcomas raised several intriguing questions. Why and how does chronic muscle regeneration in p53 germline knockouts lead to predominant formation of RMS tumors and what is in fact the cellular origin of RMS tumors? Our data clearly show that sustained activation and division of muscle SCs promotes tumorigenesis in genomically instable SCs and additionally indicates maintenance of SC quiescence as a cellular mechanism to suppress tumorigenesis. Importantly, lineage tracing enabled us (1) to determine the cancer cell of origin, (2) to prospectively purify "genuine" tumor propagating cells, and (3) to identify discrete oncogenic amplifications associated with tumor formation via genomic sequencing. Separation of tumorigenic from stromal cells, which constitute a large part of solid tumors, was especially important in this respect, because the inherent complex cellular composition of tumors and non-tumorigenic cell therein interfered with analysis of genomic sequencing data obtained from bulk samples.

The Cancer Genome Atlas Research Network continues to report genome-wide signatures of pathologically defined tumor types, but past studies have used next generation sequencing (NGS) algorithms to detect mutations of well-annotated genomic loci, exempting recently discovered genes (Roychowdhury and Chinnaiyan, 2016). Accordingly, a more recent study revealed that oncogenic BAP1 alterations in uveal melanoma are missed by NGS mutation detection algorithms used in the past and can only be detected by more recently developed sequence-assembly-based methods (Robertson et al., 2017). Moreover, precise annotation of the human genome still remains incomplete (Chen et al., 2013; Steward et al., 2017). Therefore, tumor analyses need to be constantly repeated using updated annotated genomes and refined methods, including tumor cell purification

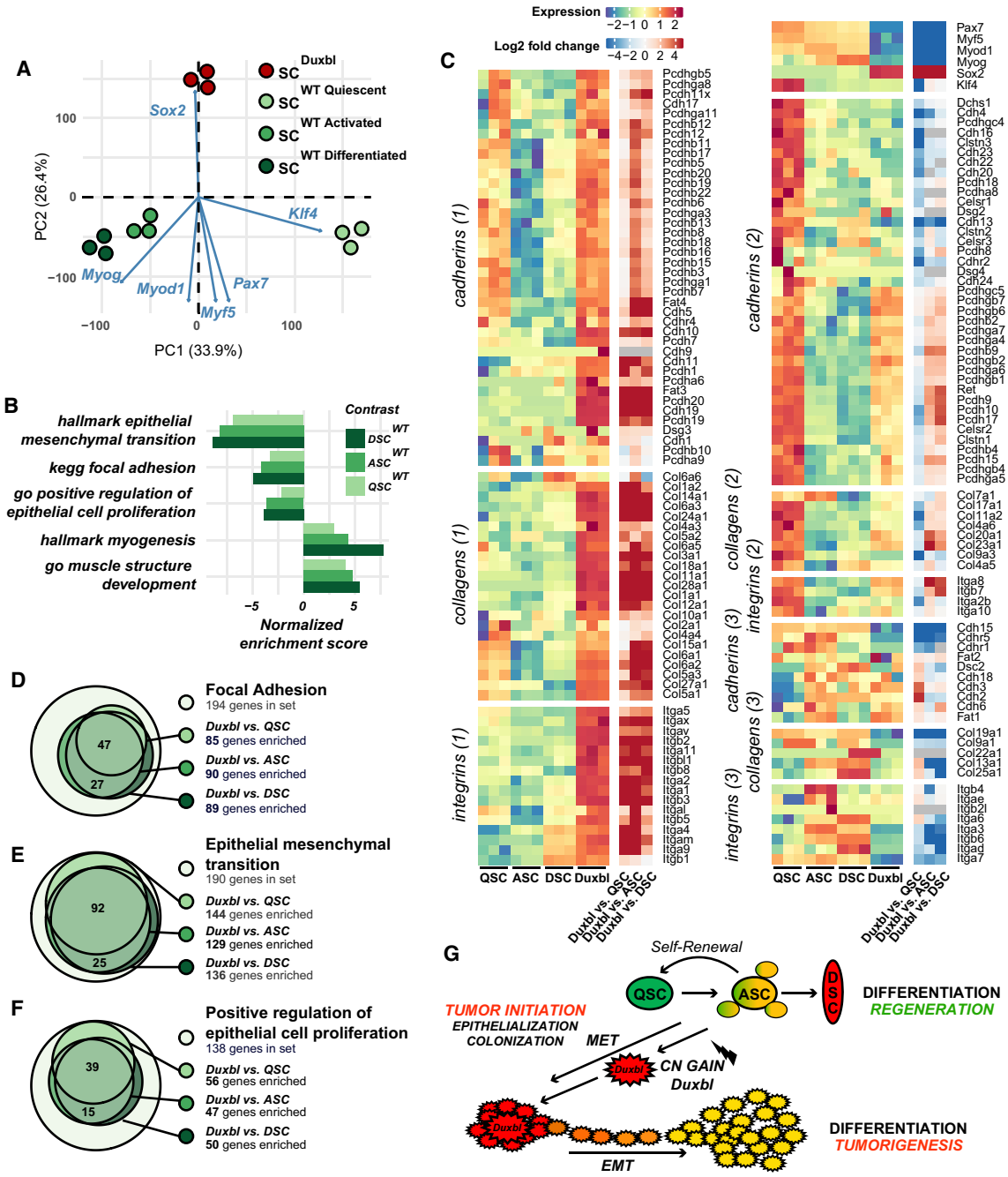

Figure 6. Overexpression of Duxbl in Muscle SCs Elicits Epithelialization

(A) Principal-component analyses of RNA-seq gene-expression data of SC^{Duxbl} and different stages of SC^{WT}.

(B and D–F) GSEA of SC^{Duxbl} and different stages of SC^{WT} with normalized enrichment score (B) and associated genes of focal adhesion (D), epithelial to mesenchymal transition (E), and regulation of epithelial cell proliferation (F).

(C) Heatmaps showing differential expression of genes driving focal adhesion, including cadherins, protocadherins, collagens, and integrins.

(G) Model depicting proposed mechanism of DuxB-Duxbl-mediated tumorigenesis. Healthy SCs contribute to muscle regeneration by differentiation of activated SCs upon injury. Copy number gain or expression of DuxB-Duxbl in activated SCs suppresses differentiation and promotes gain of SC plasticity accompanied by epithelialization and initiation of tumorigenic colonies. A secondary event likely involving EMT enables outgrowth of tumor cells from the tumor colony. ASC, activated stem cell; CN, copy number; DSC, differentiated stem cell; EMT, epithelial-to-mesenchymal transition; MET, mesenchymal-to-epithelial transition; QSC, quiescent stem cell.

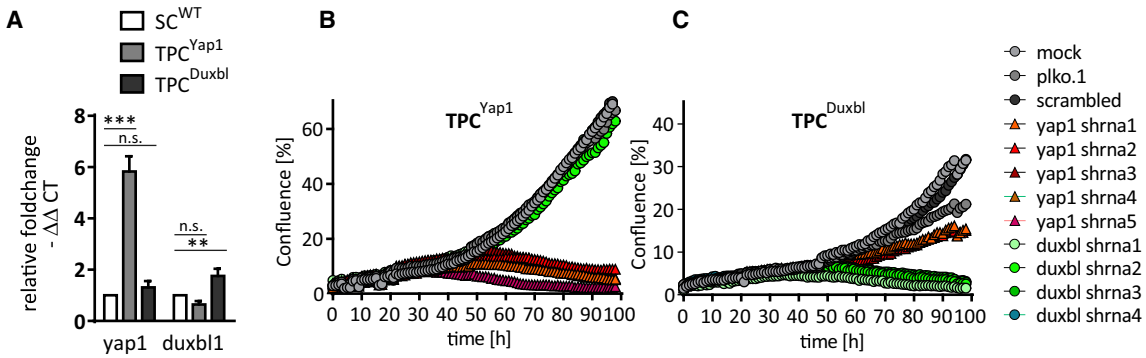

Figure 7. Targeting Duxbl

(A) qRT-PCR analysis of yap1 and duxbl in purified TPC^{Yap1} or TPC^{Duxbl}. Muscle stem cells purified from wild-type mice (SC^{WT}) served as controls. Expression levels were normalized to m36b4 mRNA. Error bars indicate SD of the mean (t test: $^{**}p < 0.01$; $^{***}p < 0.001$; n = 3).

(B and C) Growth curves of purified TPCs transduced with different shRNA lentiviruses targeting either yap1 or duxbl in TPC^{Yap1} (B) and TPC^{Duxbl} (C).

See also related videos deposited at Mendeley Data at https://doi.org/10.17632/7g2pbbrn4m.1.

or single-cell sequencing to identify new tumorigenic mutations. Here, we were able to unmask sample complexity through genomic profiling of purified TPCs, which enabled identification of distinct oncogenic amplifications in almost every analyzed animal.

Most importantly, we identified a novel oncogenic CNA of Duxbl, the murine paralog of human DuxB. Our data clearly indicate that redeployment of Dux transcription factors that define gene expression signatures of totipotent cleavage-stage ESCs (De Iaco et al., 2017; Hendrickson et al., 2017; Whiddon et al., 2017) confer stem cell expression profiles facilitating tumorigenesis in a broad range of human cancers and particularly in those of germ cell and epithelial origin. It did not miss our attention that three tumors harbored distinct copy number gains of the epigenetic regulators *smchd1* and *kdm4d* (Figure 3G), direct upstream and downstream effectors of Dux4, respectively, which indicates the Dux-ZGA axis to play a more prominent role in tumorigenesis than previously appreciated. Interestingly, derepression of silenced Dux4 in post-mitotic skeletal muscle fibers activates genes normally expressed in embryonic development and causes facioscapulohumeral muscular dystrophy (FSHD) (Lemmers et al., 2010). Ectopic expression of Dux4 in somatic cells causes cell death by yet unclarified mechanisms but seems to require a C-terminal domain specific to Dux4 that is not contained in DuxB-Duxbl (Bosnakovski et al., 2008a, 2017; Hewitt, 2015; Rickard et al., 2015). This indicates that different members of the Dux family appear to own different properties and/or exert different functions when expressed alone or with other Dux genes. In our mouse model, we observed oncogenic amplification of Duxbl, but not Dux, the human homolog of Dux4, and expression of Dux4 in human samples was almost always accompanied by co-expression of DuxB, which supports this conclusion. It is additionally tempting to speculate that higher resistance to cell death (e.g., by mutation of p53) might further render stem cells especially vulnerable to tumorigenic transformation by Dux factors.

The finding that Duxbl confers cellular plasticity and induces an MET-like process is particularly fascinating. The cancer stem cell (CSC) theory puts forward that most tumor cells lack tumor-initiating ability and that only a rare subpopulation of "stem-like" cells can lead to metastatic disease. Indeed, similar to pluripotent ESCs and iPSCs, CSCs show a plasticity that allows them to transition between epithelial- and mesenchymal-like states (Polyak and Weinberg, 2009). In accordance to the "seed and soil" hypothesis, we propose that forced expression of DuxB-Duxbl results in the initiation of a cancer stem cell that is a seed seeking the most fertile soil (a niche with constant low differentiation pressure) for it to grow in (Peinado et al., 2017). In such a scenario, it is reasonable that a chronic regeneration environment can generate focal niches that foster Duxbl-triggered MET, enabling initiation of plastic tumorigenic colonies, but a secondary event for the establishment of truly metastatic niches is likely required to enable tumor cell outgrowth (Figure 6G).

Finally, our results also revealed that inactivation of Duxbl in TPC^{Duxbl}, but not in TPC^{Yap1}, abolished tumor cell propagation and vice versa, indicating the dependence of individual tumors on distinct regulatory networks. The development of specific Dux inhibitors might allow personalized therapeutic interventions for patients suffering from Dux-factor-linked cancers, which can nowadays be easily diagnosed by sequencing approaches.

STAR★METHODS

Detailed methods are provided in the online version of this paper and include the following:

- KEY RESOURCES TABLE
- CONTACT FOR REAGENT AND RESOURCE SHARING
- EXPERIMENTAL MODEL AND SUBJECT DETAILS
  - Mice
  - Cell culture
- METHOD DETAILS
  - mRNA expression analysis
  - Immunofluorescence and immunohistochemistry
  - Knockdown by shRNA transduction
  - Exome sequencing, bioinformatics
  - Analysis of public data
- QUANTIFICATION AND STATISTICAL ANALYSIS
- DATA AND SOFTWARE AVAILABILITY

SUPPLEMENTAL INFORMATION

Supplemental Information includes seven figures and seven tables and can be found with this article online at https://doi.org/10.1016/j.stem.2018.10.011.

ACKNOWLEDGMENTS

This work was supported by the Max Planck Society, the DFG (Excellence Cluster Cardio-Pulmonary System [ECCPS]), the DFG Collaborative Research Centers SFB1213 (TP A02 and B02) and SFB TR81 (TP02), the LOEWE Center for Cell and Gene Therapy, the Foundation Leducq (3CVD01), and the German Center for Cardiovascular Research and the European Research Area Network on Cardiovascular Diseases project CLARIFY. M.G. is supported by a grant from the Herz Foundation "Infectophysics." We would like to thank J. Beetz and A. Romao for preparation of samples and help with animal work.

AUTHOR CONTRIBUTIONS

J.K. designed the study; J.P., J.Z., K.S., M.G., M.L., R.R., T.B., and J.K. interpreted and visualized data; J.P., T.E., C.K., M.L., and J.K. conducted bioinformatic analyses; J.K., J.Z., and K.S. performed experiments; S.G. performed sequencing; M.G. carried out pathological assessment; J.K. supervised the study; J.K. wrote the manuscript; and J.P., M.L., M.G., R.R., T.B., and J.K. edited the manuscript.

DECLARATION OF INTERESTS

The authors declare no competing interests.

Received: May 24, 2018
Revised: August 27, 2018
Accepted: October 8, 2018
Published: November 15, 2018

REFERENCES

Almada, A.E., and Wagers, A.J. (2016). Molecular circuitry of stem cell fate in skeletal muscle regeneration, ageing and disease. Nat. Rev. Mol. Cell Biol. *17*, 267–279.

Ben-Porath, I., Thomson, M.W., Carey, V.J., Ge, R., Bell, G.W., Regev, A., and Weinberg, R.A. (2008). An embryonic stem cell-like gene expression signature in poorly differentiated aggressive human tumors. Nat Genet. *40*, 499–507.

Blum, J.M., Añó, L., Li, Z., Van Mater, D., Bennett, B.D., Sachdeva, M., Lagutina, I., Zhang, M., Mito, J.K., Dodd, L.G., et al. (2013). Distinct and overlapping sarcoma subtypes initiated from muscle stem and progenitor cells. Cell Rep. *5*, 933–940.

Boldrin, L., Zammit, P.S., and Morgan, J.E. (2015). Satellite cells from dystrophic muscle retain regenerative capacity. Stem Cell Res. (Amst.) *14*, 20–29.

Bosnakovski, D., Lamb, S., Simsek, T., Xu, Z., Belayew, A., Perlingeiro, R., and Kyba, M. (2008a). DUX4c, an FSHD candidate gene, interferes with myogenic regulators and abolishes myoblast differentiation. Exp. Neurol. *214*, 87–96.

Bosnakovski, D., Xu, Z., Li, W., Thet, S., Cleaver, O., Perlingeiro, R.C., and Kyba, M. (2008b). Prospective isolation of skeletal muscle stem cells with a Pax7 reporter. Stem Cells *26*, 3194–3204.

Bosnakovski, D., Toso, E.A., Hartweck, L.M., Magli, A., Lee, H.A., Thompson, E.R., Dandapat, A., Perlingeiro, R.C.R., and Kyba, M. (2017). The DUX4 homeodomains mediate inhibition of myogenesis and are functionally exchangeable with the Pax7 homeodomain. J. Cell Sci. *130*, 3685–3697.

Braun, T., and Gautel, M. (2011). Transcriptional mechanisms regulating skeletal muscle differentiation, growth and homeostasis. Nat. Rev. Mol. Cell Biol. *12*, 349–361.

Camboni, M., Hammond, S., Martin, L.T., and Martin, P.T. (2012). Induction of a regenerative microenvironment in skeletal muscle is sufficient to induce embryonal rhabdomyosarcoma in p53-deficient mice. J. Pathol. *226*, 40–49.

The Cancer Genome Atlas Research Network (2017). Comprehensive and integrated genomic characterization of adult soft tissue sarcomas. Cell *171*, 950–965.e28.

Chamberlain, J.S., Metzger, J., Reyes, M., Townsend, D., and Faulkner, J.A. (2007). Dystrophin-deficient mdx mice display a reduced life span and are susceptible to spontaneous rhabdomyosarcoma. FASEB J. *21*, 2195–2204.

Chen, X., Stewart, E., Shelat, A.A., Qu, C., Bahrami, A., Hatley, M., Wu, G., Bradley, C., McEvoy, J., Pappo, A., et al.; St. Jude Children's Research Hospital–Washington University Pediatric Cancer Genome Project (2013). Targeting oxidative stress in embryonal rhabdomyosarcoma. Cancer Cell *24*, 710–724.

Davicioni, E., Anderson, M.J., Finckenstein, F.G., Lynch, J.C., Qualman, S.J., Shimada, H., Schofield, D.E., Buckley, J.D., Meyer, W.H., Sorensen, P.H., and Triche, T.J. (2009). Molecular classification of rhabdomyosarcoma–genotypic and phenotypic determinants of diagnosis: a report from the Children's Oncology Group. Am. J. Pathol. *174*, 550–564.

De Iaco, A., Planet, E., Coluccio, A., Verp, S., Duc, J., and Trono, D. (2017). DUX-family transcription factors regulate zygotic genome activation in placental mammals. Nat. Genet. *49*, 941–945.

Editorial (2015). The future of cancer genomics. Nat. Med. *21*, 99.

Donehower, L.A., Harvey, M., Slagle, B.L., McArthur, M.J., Montgomery, C.A., Jr., Butel, J.S., and Bradley, A. (1992). Mice deficient for p53 are developmentally normal but susceptible to spontaneous tumours. Nature *356*, 215–221.

Drummond, C.J., Hanna, J.A., Garcia, M.R., Devine, D.J., Heyrana, A.J., Finkelstein, D., Rehg, J.E., and Hatley, M.E. (2018). Hedgehog pathway drives fusion-negative rhabdomyosarcoma initiated from non-myogenic endothelial progenitors. Cancer Cell *33*, 108–124.e5.

Durbin, A.D., Somers, G.R., Forrester, M., Pienkowska, M., Hannigan, G.E., and Malkin, D. (2009). JNK1 determines the oncogenic or tumor-suppressive activity of the integrin-linked kinase in human rhabdomyosarcoma. J. Clin. Invest. *119*, 1558–1570.

El Demellawy, D., McGowan-Jordan, J., de Nanassy, J., Chernetsova, E., and Nasr, A. (2017). Update on molecular findings in rhabdomyosarcoma. Pathology *49*, 238–246.

Fleischmann, A., Jochum, W., Eferl, R., Witowsky, J., and Wagner, E.F. (2003). Rhabdomyosarcoma development in mice lacking Trp53 and Fos: tumor suppression by the Fos protooncogene. Cancer Cell *4*, 477–482.

Flex, E., Jaiswal, M., Pantaleoni, F., Martinelli, S., Strullu, M., Fansa, E.K., Caye, A., De Luca, A., Lepri, F., Dvorsky, R., et al. (2014). Activating mutations in RRAS underlie a phenotype within the RASopathy spectrum and contribute to leukaemogenesis. Hum. Mol. Genet. *23*, 4315–4327.

Gross, J.G., and Morgan, J.E. (1999). Muscle precursor cells injected into irradiated mdx mouse muscle persist after serial injury. Muscle Nerve *22*, 174–185.

Günther, S., Kim, J., Kostin, S., Lepper, C., Fan, C.M., and Braun, T. (2013). Myf5-positive satellite cells contribute to Pax7-dependent long-term maintenance of adult muscle stem cells. Cell Stem Cell *13*, 590–601.

Hendrickson, P.G., Doráis, J.A., Grow, E.J., Whiddon, J.L., Lim, J.W., Wike, C.L., Weaver, B.D., Pflueger, C., Emery, B.R., Wilcox, A.L., et al. (2017). Conserved roles of mouse DUX and human DUX4 in activating cleavage-stage genes and MERVL/HERVL retrotransposons. Nat. Genet. *49*, 925–934.

Hettmer, S., Liu, J., Miller, C.M., Lindsay, M.C., Sparks, C.A., Guertin, D.A., Bronson, R.T., Langenau, D.M., and Wagers, A.J. (2011). Sarcomas induced in discrete subsets of prospectively isolated skeletal muscle cells. Proc. Natl. Acad. Sci. USA *108*, 20002–20007.

Hewitt, J.E. (2015). Loss of epigenetic silencing of the DUX4 transcription factor gene in facioscapulohumeral muscular dystrophy. Hum. Mol. Genet. *24* (R1), R17–R23.

Hoadley, K.A., Yau, C., Wolf, D.M., Cherniack, A.D., Tamborero, D., Ng, S., Leiserson, M.D.M., Niu, B., McLellan, M.D., Uzunangelov, V., et al.; Cancer Genome Atlas Research Network (2014). Multiplatform analysis of 12 cancer types reveals molecular classification within and across tissues of origin. Cell *158*, 929–944.

Irintchev, A., Rosenblatt, J.D., Cullen, M.J., Zweyer, M., and Wernig, A. (1998). Ectopic skeletal muscles derived from myoblasts implanted under the skin. J. Cell Sci. *111*, 3287–3297.

Jonkers, J., Meuwissen, R., van der Gulden, H., Peterse, H., van der Valk, M., and Berns, A. (2001). Synergistic tumor suppressor activity of BRCA2 and p53 in a conditional mouse model for breast cancer. Nat. Genet. *29*, 418–425.

Kim, J., and Braun, T. (2014). Skeletal muscle stem cells for muscle regeneration. Methods Mol. Biol. *1213*, 245–253.

Kim, J.B., Sebastiano, V., Wu, G., Araúzo-Bravo, M.J., Sasse, P., Gentile, L., Ko, K., Ruau, D., Ehrich, M., van den Boom, D., et al. (2009). Oct4-induced pluripotency in adult neural stem cells. Cell *136*, 411–419.

Leidenroth, A., and Hewitt, J.E. (2010). A family history of DUX4: phylogenetic analysis of DUXA, B, C and Duxbl reveals the ancestral DUX gene. BMC Evol. Biol. *10*, 364.

Leidenroth, A., Clapp, J., Mitchell, L.M., Coneyworth, D., Dearden, F.L., Iannuzzi, L., and Hewitt, J.E. (2012). Evolution of DUX gene macrosatellites in placental mammals. Chromosoma *121*, 489–497.

Lemmers, R.J., van der Vliet, P.J., Klooster, R., Sacconi, S., Camaño, P., Dauwerse, J.G., Snider, L., Straasheijm, K.R., van Ommen, G.J., Padberg, G.W., et al. (2010). A unifying genetic model for facioscapulohumeral muscular dystrophy. Science *329*, 1650–1653.

Lepper, C., Conway, S.J., and Fan, C.M. (2009). Adult satellite cells and embryonic muscle progenitors have distinct genetic requirements. Nature *460*, 627–631.

Li, R., Liang, J., Ni, S., Zhou, T., Qing, X., Li, H., He, W., Chen, J., Li, F., Zhuang, Q., et al. (2010). A mesenchymal-to-epithelial transition initiates and is required for the nuclear reprogramming of mouse fibroblasts. Cell Stem Cell *7*, 51–63.

Liu, C., Li, D., Hu, J., Jiang, J., Zhang, W., Chen, Y., Cui, X., Qi, Y., Zou, H., Zhang, W., and Li, F. (2014). Chromosomal and genetic imbalances in Chinese patients with rhabdomyosarcoma detected by high-resolution array comparative genomic hybridization. Int. J. Clin. Exp. Pathol. *7*, 690–698.

Madissoon, E., Jouhilahti, E.M., Vesterlund, L., Töhönen, V., Krjutškov, K., Petropoulos, S., Einarsdottir, E., Linnarsson, S., Lanner, F., Månsson, R., et al. (2016). Characterization and target genes of nine human PRD-like homeobox domain genes expressed exclusively in early embryos. Sci. Rep. *6*, 28995.

Morrison, S.J., and Spradling, A.C. (2008). Stem cells and niches: mechanisms that promote stem cell maintenance throughout life. Cell *132*, 598–611.

Peinado, H., Zhang, H., Matei, I.R., Costa-Silva, B., Hoshino, A., Rodrigues, G., Psaila, B., Kaplan, R.N., Bromberg, J.F., Kang, Y., et al. (2017). Pre-metastatic niches: organ-specific homes for metastases. Nat. Rev. Cancer *17*, 302–317.

Polotskaia, A., Xiao, G., Reynoso, K., Martin, C., Qiu, W.G., Hendrickson, R.C., and Bargonetti, J. (2015). Proteome-wide analysis of mutant p53 targets in breast cancer identifies new levels of gain-of-function that influence PARP, PCNA, and MCM4. Proc. Natl. Acad. Sci. USA *112*, E1220–E1229.

Polyak, K., and Weinberg, R.A. (2009). Transitions between epithelial and mesenchymal states: acquisition of malignant and stem cell traits. Nat. Rev. Cancer *9*, 265–273.

Rickard, A.M., Petek, L.M., and Miller, D.G. (2015). Endogenous DUX4 expression in FSHD myotubes is sufficient to cause cell death and disrupts RNA splicing and cell migration pathways. Hum. Mol. Genet. *24*, 5901–5914.

Robertson, A.G., Shih, J., Yau, C., Gibb, E.A., Oba, J., Mungall, K.L., Hess, J.M., Uzunangelov, V., Walter, V., Danilova, L., et al. (2017). Integrative analysis identifies four molecular and clinical subsets in uveal melanoma. Cancer Cell *32*, 204–220.e15.

Roychowdhury, S., and Chinnaiyan, A.M. (2016). Translating cancer genomes and transcriptomes for precision oncology. CA Cancer J. Clin. *66*, 75–88.

Sato, Y., Yoshizato, T., Shiraishi, Y., Maekawa, S., Okuno, Y., Kamura, T., Shimamura, T., Sato-Otsubo, A., Nagae, G., Suzuki, H., et al. (2013). Integrated molecular analysis of clear-cell renal cell carcinoma. Nat. Genet. *45*, 860–867.

Shern, J.F., Chen, L., Chmielecki, J., Wei, J.S., Patidar, R., Rosenberg, M., Ambrogio, L., Auclair, D., Wang, J., Song, Y.K., et al. (2014). Comprehensive genomic analysis of rhabdomyosarcoma reveals a landscape of alterations affecting a common genetic axis in fusion-positive and fusion-negative tumors. Cancer Discov. *4*, 216–231.

Shima, N., Alcaraz, A., Liachko, I., Buske, T.R., Andrews, C.A., Munroe, R.J., Hartford, S.A., Tye, B.K., and Schimenti, J.C. (2007). A viable allele of Mcm4 causes chromosome instability and mammary adenocarcinomas in mice. Nat. Genet. *39*, 93–98.

Soini, Y., Kosma, V.M., and Pirinen, R. (2015). KDM4A, KDM4B and KDM4C in non-small cell lung cancer. Int. J. Clin. Exp. Pathol. *8*, 12922–12928.

Steward, C.A., Parker, A.P.J., Minassian, B.A., Sisodiya, S.M., Frankish, A., and Harrow, J. (2017). Genome annotation for clinical genomic diagnostics: strengths and weaknesses. Genome Med. *9*, 49.

Taulli, R., Scuoppo, C., Bersani, F., Accornero, P., Forni, P.E., Miretti, S., Grinza, A., Allegra, P., Schmitt-Ney, M., Crepaldi, T., and Ponzetto, C. (2006). Validation of met as a therapeutic target in alveolar and embryonal rhabdomyosarcoma. Cancer Res. *66*, 4742–4749.

Tomasetti, C., and Vogelstein, B. (2015). Cancer etiology. Variation in cancer risk among tissues can be explained by the number of stem cell divisions. Science *347*, 78–81.

Tremblay, A.M., Missiaglia, E., Galli, G.G., Hettmer, S., Urcia, R., Carrara, M., Judson, R.N., Thway, K., Nadal, G., Selfe, J.L., et al. (2014). The Hippo transducer YAP1 transforms activated satellite cells and is a potent effector of embryonal rhabdomyosarcoma formation. Cancer Cell *26*, 273–287.

Wang, Y., Marino-Enriquez, A., Bennett, R.R., Zhu, M., Shen, Y., Eilers, G., Lee, J.C., Henze, J., Fletcher, B.S., Gu, Z., et al. (2014). Dystrophin is a tumor suppressor in human cancers with myogenic programs. Nat. Genet. *46*, 601–606.

Whiddon, J.L., Langford, A.T., Wong, C.J., Zhong, J.W., and Tapscott, S.J. (2017). Conservation and innovation in the DUX4-family gene network. Nat. Genet. *49*, 935–940.

Williamson, D., Missiaglia, E., de Reyniès, A., Pierron, G., Thuille, B., Palenzuela, G., Thway, K., Orbach, D., Laé, M., Fréneaux, P., et al. (2010). Fusion gene-negative alveolar rhabdomyosarcoma is clinically and molecularly indistinguishable from embryonal rhabdomyosarcoma. J. Clin. Oncol. *28*, 2151–2158.

Wüst, S., Dröse, S., Heidler, J., Wittig, I., Klockner, I., Franko, A., Bonke, E., Günther, S., Gärtner, U., Boettger, T., et al. (2018). Metabolic Maturation during Muscle Stem Cell Differentiation Is Achieved by miR-1/133a-Mediated Inhibition of the Dlk1-Dio3 Mega Gene Cluster. Cell Metab. *27*, 1026–1039.e6.